Publ. Astron. Soc. Japan 35, 91–100 (1983)

The Radio Continuum Loop G56+14 Possibly Associated with an H I Shell

Yoshiaki SOFUE

Nobeyama Radio Observatory, Nobeyama, Minamimaki-mura, Minamisaku-gun, 384-13 Nagano*

(Received 1982 July 24; accepted 1982 August 23)

Abstract

A radio continuum loop of diameter 10° centered on $l=56°$, $b=14°$ was found in the 408- and 820-MHz survey data, which we hereafter call G56+14. The loop is possibly associated with an H I (neutral hydrogen) shell at a radial velocity 25 km s^{-1} (LSR) having similar characteristics to a Heiles H I shell. The distance to G56+14 is estimated as 1.9 kpc, and its linear diameter and height from the galactic plane as 330 and 470 pc, respectively. The loop is reasonably interpreted as a very old ($\sim 10^7$ yr) supernova remnant of initial explosion energy $\sim 2\times 10^{50}$ erg. Such an old SNR may still survive, not losing its identity, if an interstellar medium in the interarm region at this height ($\sim$0.5 kpc) is "quiet" or less turbulent compared with the near-plane medium.

Key words: H I emission; Interstellar medium; Radio continuum emission; Radio loops; Supernova remnants.

1. Introduction

Low-brightness and large-diameter supernova remnants (SNR) other than the so far detected SNRs may possibly be hidden in the complicated and fluctuated radio continuum background of the Galaxy. Such loops, if identified, will provide another mean to investigate the late-stage evolution of SNRs, their birth rate in the Galaxy, and the physical state of the interstellar medium.

The detection of a number of neutral hydrogen (H I) shells by Heiles (1979) and Hu (1981) has given an important clue to such large diameter objects. If the H I shells are due to explosive phenomena like supernovae, they may be associated with radio continuum emission. However, the association is not clear as yet. It is therefore worthwhile to search for radio continuum counterparts to the H I shells more carefully.

In these contexts a systematic search for radio continuum loops of medium size, namely of diameters between $\sim 4°$ and $\sim 20°$ was made using published radio continuum data. In the course of this survey work, we have noticed a prominent radio loop of 10° diameter associated with an H I shell of the same diameter. We report here this newly discovered loop object. A detailed description of the result of the systematic search for radio loops is given in a separate paper (Sofue and Nakai 1983).

2. Radio Loop G56+14 and an Associated H I Shell

(*a*) *Radio Continuum Maps and a Background-Filtering Technique*

A systematic search for loop-like structures in the radio continuum background emis-

* Nobeyama Radio Observatory is a branch of the Tokyo Astronomical Observatory, University of Tokyo.

sion has been made using the Bonn 408-MHz survey of Haslam et al. (1974) taken with the 100-m telescope and the Leiden 820-MHz survey of Berkhuijsen (1972) taken with the 25-m telescope. We applied to the data a "background filtering (BGF)" method as proposed by Sofue and Reich (1979). With this technique we can abstract structures with angular scale sizes smaller than a certain beam width Θ by filtering out scale structures larger than Θ. The method is useful to search for low-brightness and small-scale (compared with Θ) objects that are hidden or merged by a strong background radio emission with a steep intensity gradient like that due to the galactic disk component.

The BGF method is briefly summarized as follows. Suppose that the original map (map 1) was observed with a HPBW$=\theta$. We smooth the map with a wider Gaussian beam of HPBW Θ ($>\theta$) to get map 2. Then we subtract the smoothed map (map 2) from the original (map 1). The difference (map 1 minus map 2) is then subtracted from the original map only in regions where the difference is positive, yielding map 3; in map 3 the excess brightness over the smoothed brightness (map 2) has been cut off from the original. Map 3 is again smoothed to Θ to get map 4. Excesses in map 3 over map 4 are again subtracted from map 3 to get map 5, which is again smoothed to Θ. We repeat this procedure to obtain the final smoothed map which contains structures of scale sizes larger than Θ and traces the "smooth lower envelope" of the original map. The "smooth lower envelope" is finaly subtracted from the original (map 1) and we obtain a map for our purpose which contains only structures with scale sizes between θ and Θ. A detailed description of the BGF method and some results by use of this technique are given in Sofue and Reich (1979).

We have applied the BGF method to the Bonn 408-MHz survey data (Haslam et al. 1974) and to the Leiden 820-MHz survey data (Berkhuijsen 1972). The resulting maps cover a wide area in the northern sky, and have revealed a number of interesting features like loop structures, arcs, and extended complicated features. We have also examined H I gas distribution around the structures thus found. About ten loops have been proved to be apparently associated with H I shells. Among them the most prominent loop has a diameter of 10° centered on $l=56°$ and $b=14°$, which we report in the present paper. Other loops and associated H I features are reported in Sofue and Nakai (1983).

(*b*) *Radio Loop G56+14*

Figure 1 shows a region of $20°\times20°$ on the sky in the galactic coordinate system centered on $l=55°$, $b=15°$. Figure 1a is an original map of the region reproduced from Haslam et al. (1971), while figure 1b was obtained by applying the BGF method to the same data. Figure 2a shows the same region as appeared in the original 820-MHz map from Berkhuijsen (1972) and figure 2b was obtained by applying the BGF method. The HPBW of the original 408-MHz map is 0°.6 and that of the 820-MHz map is 1°.2. The data reduction was made in part by making use of the NOD 2 radio astronomical reduction system (Haslam 1974). At both frequencies we have taken the smoothing beam width of $\Theta=4°$, so that structures with scale sizes smaller than 4° are emphasized. We have also examined cases taking different beam widths, which show essentially the same features as in figures 1 and 2 in so far as the beam is taken as $3°\lesssim\Theta\lesssim6°$.

If we compare figure 1a with 1b or figure 2a with 2b, we see how the BGF method is effective to find faint and extended features which are merged in the complicated, fluctuated background radio emission. However, we must be careful that, although the present technique is effective to demonstrate such faint features, the brightness temperatures on the resulting map do not necessarily represent their real figures, giving always underestimated values.

In the central region of figures 1 and 2 we find a prominent loop-like association of radio

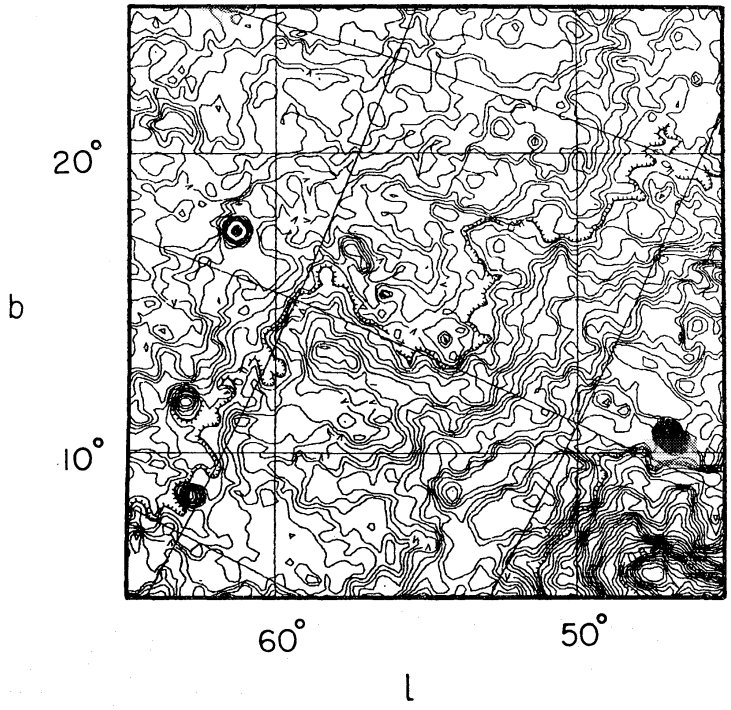

(a)

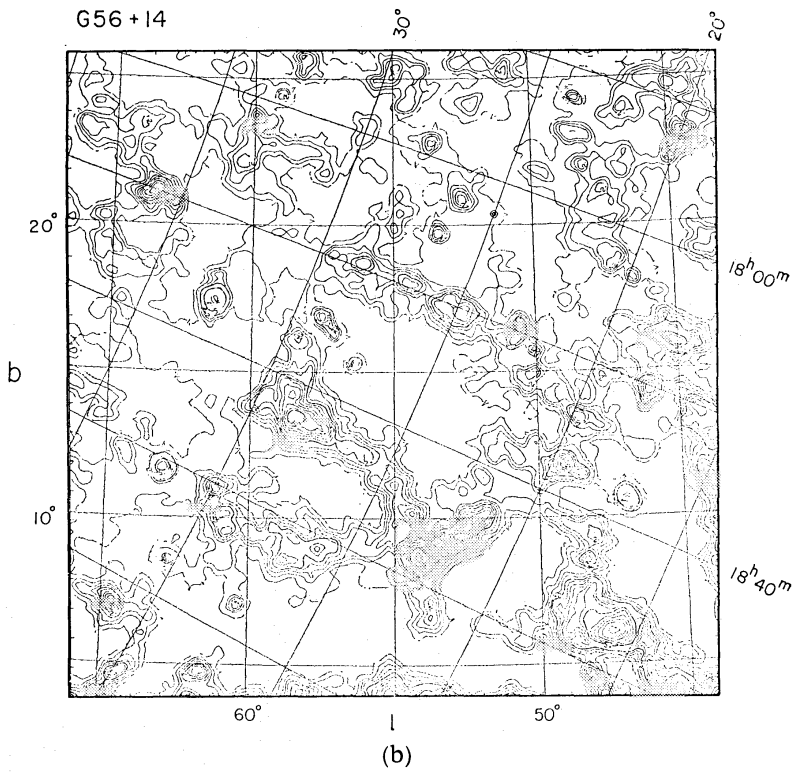

(b)

Fig. 1. (a) A part of the original map of 408-MHz Bonn survey reproduced from Haslam et al. (1974). The HPBW is 0°.6. The contours represent brightness temperature at intervals of 1K. (b) A 408-MHz map obtained by applying the "background filtering (BGF)" method with $\Theta=4°$ to the Bonn survey data in figure 1a. The contours show the brightness temperature at intervals of 0.5K. A loop-like structure is found centered on $l=56°$, $b=14°$ with a diameter of 10°, which we call the radio loop G56+14.

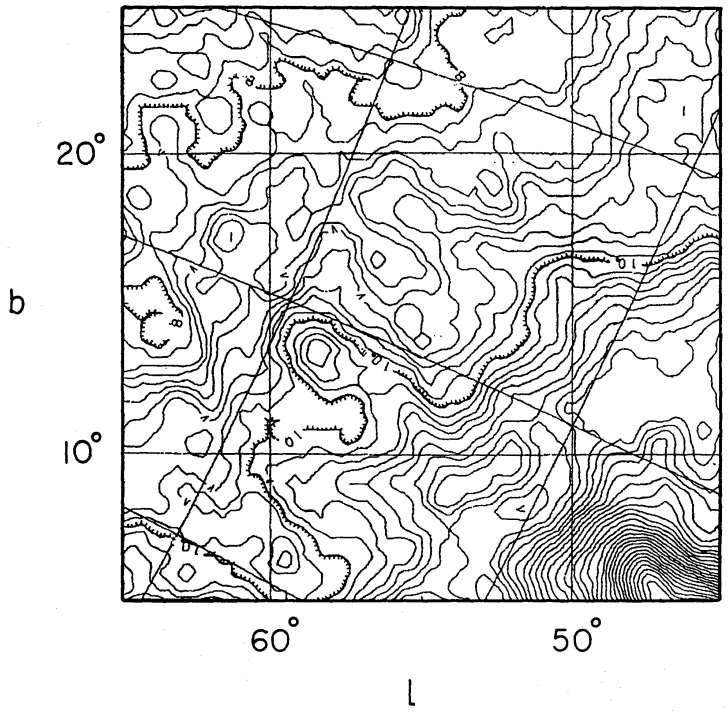

(a)

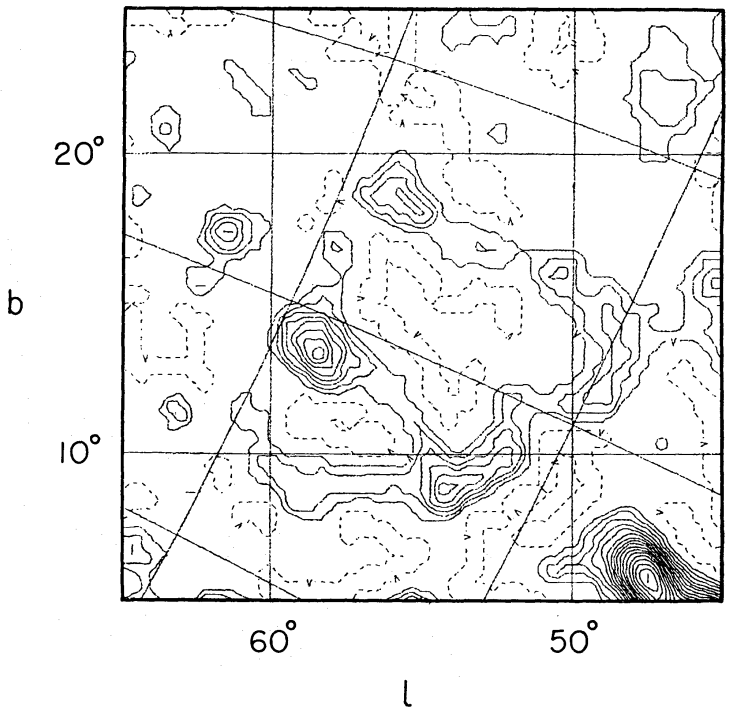

(b)

Fig. 2. (a) The same region as in figure 1 but for the original 820-MHz map reproduced from the Leiden survey by Berkhuijsen (1972). The contours are brightness temperature at interval of 0.2K. The HPBW is 1°.2. (b) A 820-MHz map obtained by applying the BGF method with $\Theta=4°$ to the Leiden survey data in figure 2a. The contours represent the brightness temperature at interval of 0.1 K. The dashed contours are at 0 K.

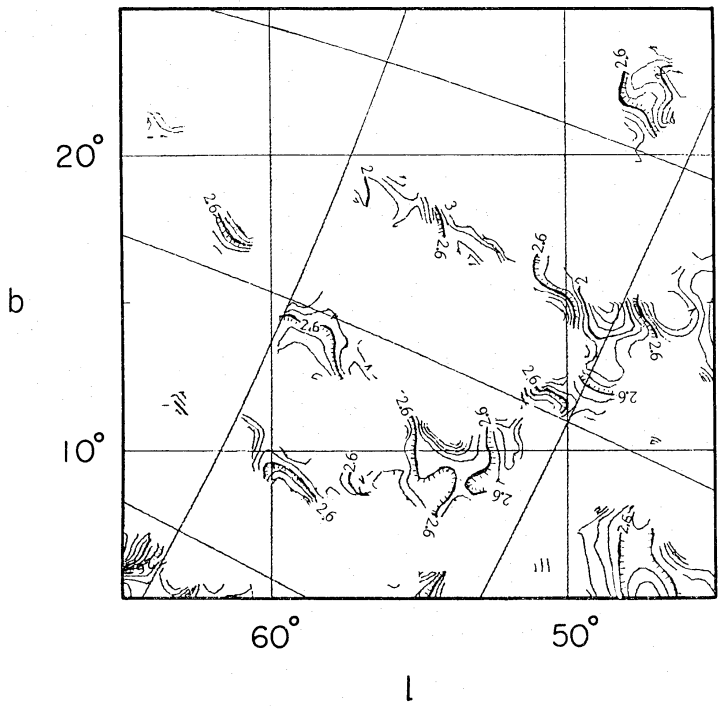

Fig. 3. The distribution of spectral index ($-\beta$) of brightness temperature obtained from the 408- and 820-MHz survey data after smoothing the original maps to a HPBW of 1°.3 and then applying the BGF method with $\Theta=4°$. The contours at $\beta=-2.6$ are hatched on the more positive-β (more thermal) side. The error in β is typically ± 0.4.

ridges with a diameter of approximately 10° and its center on $l=56°$, $b=14°$. We hereafter call this loop-like structure G56+14. The excess brightness of the loop ridges over the background is 2–4 K at 408 MHz and 0.3–0.6 K at 820 MHz. The loop ridge involves many point-like sources with peak brightness temperatures of 2–5 K at 408 MHz. We also find that a bright ridge runs from $l=59°$, $b=14°$ toward the south, cutting across the loop.

Figure 3 shows the distribution of spectral index β derived from the 408- and 820-MHz maps, where β is defined through $T_b^{820}/T_b^{408}=(820/408)^{\beta}$ with T_b^{ν} the brightness temperature at ν MHz. The spectral index was calculated after smoothing the original maps at 408 and 820 MHz both to HPBW of 1°.3 and then applying the BGF method with $\Theta=4°$. The index is given only for regions where the brightness at 408 MHz is higher than 0.4 K and that at 820 MHz is higher than 0.1 K. The error in β is estimated through

$$\Delta\beta \approx [(\Delta T_b/T_b)^2_{408}+(\Delta T_b/T_b)^2_{820}]^{1/2}/\ln(820/408), \quad (1)$$

where ΔT_b is the error in T_b and is mainly determined by the background subtraction through the BGF method. We estimate that $\Delta T_b/T_b \approx 0.2$ for both frequencies, which leads to $\Delta\beta \approx 0.4$. The figure shows that the loop ridges have spectral index of $\beta=-2.4$ to -3.0, typically -2.6. We may therefore conclude that G56+14 is of nonthermal origin.

(c) *Some Other Features*

We mention the following two other features found in figure 1b: A deformed loop-like feature is found centered on $l=52°$, $b=8°$ with a diameter of $\sim 5°$. In positional coincidence with this feature we know an H I shell, G52+07+39, whose distance is 3.1 kpc and the diameter 300 pc (Heiles 1979). However, it is still difficult to judge if this is really associated with the radio loop feature, because the radio loop is too much deformed and does not fit the H I shape (figure 4).

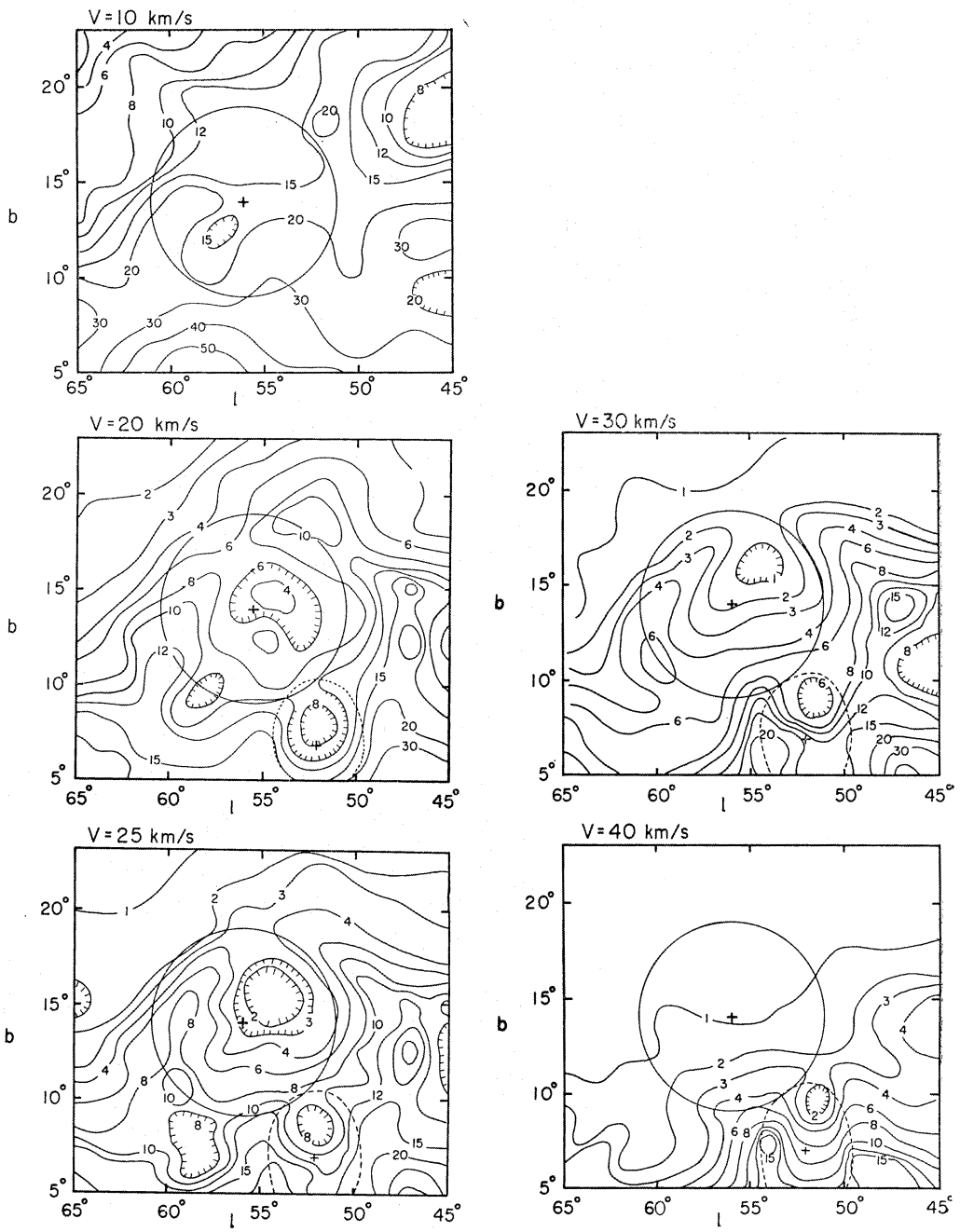

Fig. 4. Antenna temperatures of the H I-line emission at velocities (LSR) of (a) 10 km s^{-1}, (b) 20 km s^{-1}, (c) 25 km s^{-1}, (d) 30 km s^{-1}, and (e) 40 km s^{-1}. The contour units are in kelvins. An H I shell associated with the radio loop G56+14 (indicated with a circle) is found at velocities 20–30 km s^{-1}. A Heiles H I shell, G52+07+39, is indicated with the dashed lines.

A partially loop-like radio enhancement of diameter $\sim 3°$ is found at the lower-left corner of figure 1b centered on $l=65°$, $b=6°$. This is a recently discovered supernova remnant G65.2+05.7 both in optical and radio continuum emission (Gull et al. 1977; Reich et al. 1979). Its diameter is estimated to be 75 pc, distance 0.9 kpc, the height from the

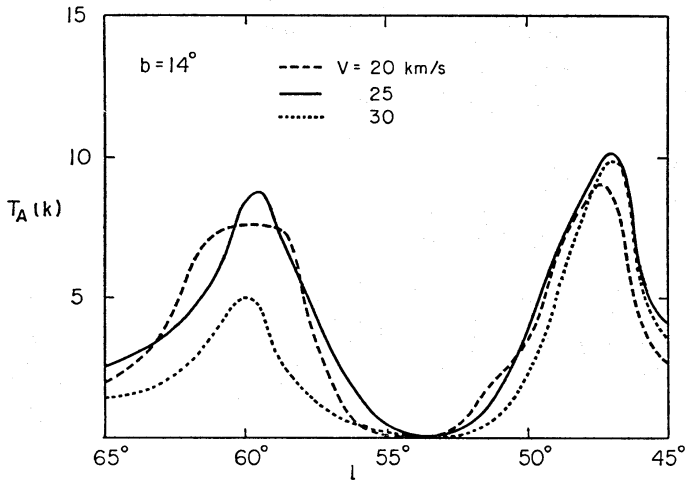

Fig. 5. Cross cuts of the H I shell associated with G56+14 at $V=20$ (dashed line), 25 (full line), and 30 km s^{-1} (dotted line) at a constant latitude, $b=14°$. The base lines have been subtracted by assuming a linear slope.

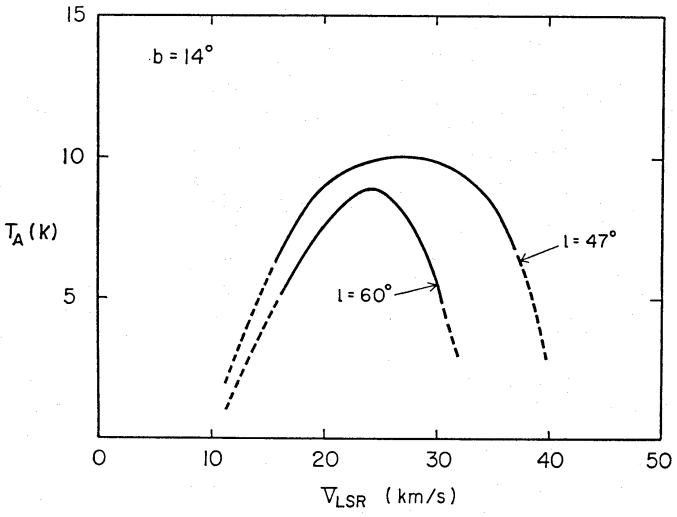

Fig. 6. Variations of the antenna temperature of the H I-line emission at $l=47°$, $b=14°$ (southern ridge of the H I shell) and at $l=60°$, $b=14°$ (northern ridge) against the radial velocity V in LSR.

galactic plane approximately 90 pc, and the age is estimated to be 2.4×10^5 yr (Reich et al. 1979).

(*d*) *An H I Shell Associated with the Radio Loop G56+14*

In order to examine any association of an H I feature with the radio loop G56+14, we make several maps of H I gas distributions (figure 4) at various velocities for the same region as in figures 1 and 2, using the H I survey data by Weaver and Williams (1973, 1974) and Heiles and Habing (1974). In a good positional coincidence with the radio loop, we find a loop-shaped H I ridge centered on $l=55°$, $b=15°$ with a diameter of approximately 11° in the H I maps at $V=20$, 25, and 30 km s^{-1}. The H I loop feature can be recognized in the maps in a velocity range from 15 to 35 km s^{-1}, while it disappears at $V<15$ km s^{-1} and $V>35$ km s^{-1} [see also Colomb et al. (1980)].

Figure 5 shows cross cuts of the H I maps for $V=20$, 25, and 35 km s^{-1} at a constant

latitude, $b=14°$, crossing the center of G56+14, where the base lines have been subtracted assuming that they have linearly varying slopes against the longitude. Figure 6 shows the variation of the antenna temperature at $l=47°$ and 60° both at $b=14°$ as a function of the radial velocity. From the figure we see that the H I loop has a mean radial velocity of 25 ± 3 km s^{-1} and the velocity dispersion in the loop ridge is of the order of 15 km s^{-1}.

Comparing figures 5 and 6 as well as the maps in figure 4, we may conclude that the loop is in a stationary state; there is no evidence for expanding motion greater than 10 km s^{-1}. This H I loop may be a "stationary shell" in terms of Heiles' (1979) categorization.

4. Discussion

(a) *Kinematical Distance, Diameter, and H I Mass of G56+14*

If the neutral hydrogen shell is physically associated with G56+14 and obeys the galactic circular rotation, its distance is estimated to be 1.9 ± 0.5 kpc from its radial velocity, 25 km s^{-1}. The linear diameter is then estimated as 330 ± 80 pc by combining the distance with the angular diameter of 11°. The linear shell thickness is about 60 pc from the apparent thickness of 2°. Using these parameters and the peak antenna temperature of 8K together with the velocity width typically taken as 15 km s^{-1}, we obtain the approximate H I mass of the shell to be $\sim2\times10^4\,M_\odot$. This is well in the range of the masses of the H I shells (Heiles 1979). The parameters for the radio loop G56+14 and for the associated H I shells are

Table 1. Parameters for the radio loop G56+14.

Radio loop	
Position	R.A.(1950)=18^{h}40^m, Decl.(1950)=26.5°
	$l=56°$, $b=14°$
Angular diameter	$\theta_R\cong10°$
Loop width	$w_R\cong2°$
Mean brightness temperature over loop the	T_b(408 MHz)$\sim$0.5 K
	T_b(820 MHz)$\sim$0.1 K
Surface brightness over the loop	Σ(408 MHz)$\sim2\times10^{-23}$ Wm^{-2} Hz^{-1} sr^{-1}
	Σ(820 MHz)$\sim1.3\times10^{-23}$ Wm^{-2} Hz^{-1} sr^{-1}
H I shell	
Position	R.A.(1950)=18^{h}30^m, Decl.(1950)=26°
	$l=55°$, $b=15°$
Angular diameter	$\theta_{HI}\cong11°$
Shell width	$w_{HI}\cong2°$
Central radial velocity (LSR)	$V=25$ km s^{-1}
Expansion velocity	$V_{sh}\lesssim10$ km s^{-1}
Velocity width	$\sigma_v\cong15$ km s^{-1}
Antenna temperature on the shell ridge	$T_A\cong8$ K
Derived quantities	
Distance	$d=1.9\pm0.5$ kpc
Diameter	$D=330\pm80$ pc
Height from the galactic plane	$z=470\pm120$ pc
Shell thickness	$W_{HI}=70\pm18$ pc
H I mass	$M_{HI}\sim2\times10^4\,M_\odot$
Ambient gas density	$n_0\sim0.03$ cm^{-3}
Explosion energy	$E\sim2\times10^{50}$ erg
Time scale (age)	$t\sim2\times10^7$ yr

summarized in table 1 together with some quantities derived for G56+14 which is assumed to be an old SNR.

We note that the velocity difference in the northern and southern parts of the H I shell can be attributed to the galactic differential rotation; the radial velocity of the ridge at $l=47°$ is $V=28$ km s^{-1} and that at $l=60°$ is 24 km s^{-1} (figure 6). Indeed the calculated radial velocities due to the galactic rotation at $l=47°$ and 60° at a distance of 1.9 kpc are 27 and 23 km s^{-1}, respectively, which are in good agreement with the observed peak velocities. This fact is again consistent with the idea that the shell is not in a dynamical state but in a stationary state obeying the galactic rotation.

(*b*) *Origin and Total Energy of Explosion*

If the radio loop G56+14 is a similar object to a Heiles H I shell and located at a distance of 1.9 kpc, we can estimate its total energy of initial explosion by applying the following equation obtained for a late stage of the SNR evolution (Chevalier 1974; Heiles 1979):

$$E=5.3\times10^{43}\, n_0^{1.12} R^{3.12} V^{1.4}\ \text{erg}\,, \qquad (1)$$

where n_0 is the ambient gas density in cubic centimeters, R is the radius of the shell in parsecs, and V is the expansion velocity of the shell in units of km s^{-1}. We may assume that the shell of SNR in as late a stage of evolution as that of G56+14 has been already stopped by the interstellar medium and the expansion velocity of the shell has become equal to the sound velocity of the medium of 10 km s^{-1} (see figure 5). If we assume that the H I mass involved in the shell has been swept up from the volume of radius R, then we may estimate n_0 through $M_{\rm HI}\sim(4\pi/3)R^3 n_0 m_{\rm H}$ with $m_{\rm H}$ the hydrogen atom mass. Taking $M\sim2\times10^4 M_\odot$ and $R\sim160$ pc, we have $n_0\sim0.03$ cm^{-3}. Now we can estimate the total energy from the above equation to obtain $E\sim2\times10^{50}$ erg. This is a typical value of the explosion energy of a type II supernova.

(*c*) *An Extremely Old SNR?*

The estimated explosion energy as well as the fact that it is a radio loop seems to be consistent with the view that G56+14 is a very old SNR. The age is then estimated to be of the order of $t\sim R/V_{\rm sh}\sim2\times10^7$ yr by taking $V_{\rm sh}\sim10$ km s^{-1}. The radio surface brightness of G56+14 is lower than any SNRs so far cataloged, and the size is larger than any of them (Milne 1979). We note that the diameter of G56+14, $D\sim330$ pc, is even larger than those estimated for the galactic radio loops I–IV, if the loops are attributed to supernova remnants (e. g., Berkhuijsen et al. 1971; Sofue et al. 1974). Then the radio loop G56+14 is the oldest radio SNR and its diameter is the largest among the known SNRs. G56+14 is likely to be a very old radio SNR filling the gap between the number of observed SNRs and that expected from the birth rate of SNRs in the Galaxy.

We inspected the Palomar Sky Survey prints for associated optical nebulosities. However, we could not find any optical counterpart. The large angular diameter may make it difficult to distinguish some extended, low-brightness nebulosities. No strong X-ray enhancement is found toward G56+14 in the energy range of 0.1–1 keV (McCammon 1979).

(*d*) *"Quiet" Interstellar Medium Surrounding G56+14*

Now a question may arise: why can an SNR in a such late stage of evolution ($\sim10^7$ yr) still survive not losing its identity as a loop? This may be due to a relatively low-density, quiet ambient medium, which may be realized at its height, $z\sim0.5$ kpc, and in the inter-arm region between Cygnus and Sagittarius arms, where G56+14 is located. A low birth rate

of SNs in such a high z region will cause a less turbulent state in the ambient medium than that in the of regions lower altitude and/or near the spiral arm.

From a plot of numbers of SNRs at distances less than 10 kpc from the Sun against their heights from the galactic plane using an SNR catalog given by Milne (1979), we obtain that the number of SNRs varies with the height z as

$$N(>|z|)=N_0 \exp(-|z|/100 \text{ pc}), \quad (2)$$

where N_0 is a constant. If we assume the birth rate of SNRs in our Galaxy as 1 per ~ 30 yr (Milne 1979), N_0 for SNRs with the age less than $\sim 10^7$ yr is calculated to be $N_0=10^3$ kpc^{-2}. Then we have the number of SNRs which exploded at $z \gtrsim 470$ pc and with the age of $t \sim 10^7$ yr to be $N \sim 10$ kpc^{-2}. If we recall that G56+14 is located at the inter-arm, this number will be much smaller: $N \sim$ a few kpc^{-2}. This is small enough so that the SNRs do not disturb one another. On the other hand, SNRs born at lower altitudes and/or near the spiral arms should be more disturbed by one another as well as by the denser and more turbulent ambient medium. This will make it difficult to distinguish an old, low-brightness, expanded SNR at lower latitudes, say at $|b| \lesssim 10°$, especially near the spiral arms.

This research has been in part supported by the Scientific Research Fund of the Ministry of Education, Science, and Culture under Grant No. 542003 (FY1980, 1981). The numerical computations were performed on a FACOM-M200 at the Institute of Plasma Physics, Nagoya University.

References

Berkhuijsen, E. M. 1972, *Astron. Astrophys. Suppl.*, **5**, 263.
Berkhuijsen, E. M., Haslam, C. G. T., and Salter, C. J. 1971, *Astron. Astrophys.*, **14**, 252.
Chevalier, R. A. 1974, *Astrophys. J.*, **188**, 501.
Colomb, F. R., Pöppel, W. G. L., and Heiles, C. 1980, *Astron. Astrophys. Suppl.*, **40**, 47.
Gull, T. R., Kirshner, R. P., and Parker, R. A. R. 1977, *Astrophys. J. Letters*, **215**, L69.
Haslam, C. G. T. 1974, *Astron. Astrophys. Suppl.*, **15**, 333.
Haslam, C. G. T., Wilson, W. E., Graham, D. A., and Hunt, G. C. 1974, *Astron. Astrophys. Suppl.*, **13**, 359.
Heiles, C. 1979, *Astrophys. J.*, **229**, 533.
Heiles, C., and Habing, H. J. 1974, *Astron. Astrophys. Suppl.*, **14**, 1.
Hu, E. M. 1981, *Astrophys. J.*, **248**, 119.
McCammon, D. 1979, in *Symposium on the Results and Future Prospects of X-ray Astronomy* (Institute of Space and Aeronautical Science, University of Tokyo), p. 169.
Milne, D. K. 1979, *Australian J. Phys.*, **32**, 83.
Reich, W., Berkhuijsen, E. M., and Sofue, Y. 1979, *Astron. Astrophys.*, **72**, 270.
Sofue, Y., Hamajima, K., and Fujimoto, M. 1974, *Publ. Astron. Soc. Japan*, **26**, 399.
Sofue, Y., and Nakai, N. 1983. *Astron. Astrophys.*, in press.
Sofue, Y., and Reich, W. 1979, *Astron. Astrophys. Suppl.*, **38**, 251.
Weaver, H., and Williams, D. R. W. 1973, *Astron. Astrophys. Suppl.*, **8**, 1.
Weaver, H., and Williams, D. R. W. 1974, *Astron. Astrophys. Suppl.*, **17**, 1.